

assume that any single value of  $\alpha$  will be generally applicable for protein electron-transfer reactions.

**Acknowledgment.** This work was supported by grants from the N.I.H. and N.S.F. (to G.M.) and by the Office of Basic Energy

Sciences, Division of Chemical Sciences, under US-DOE contract W-31-109-ENG-38 (J.M.). We gratefully acknowledge the assistance of Ken Simolo and the ongoing advice and collaboration of Prof. Grant Mauk. Thoughtful criticisms and suggestions by Harry Gray are gratefully acknowledged.

## Laser Flash Photolysis Study of the Hydrogen Atom Transfer Reaction from Triplet 1-Naphthol to Ground Benzophenone<sup>1</sup>

Haruo Shizuka,\* Hiroyuki Hagiwara, and Masaru Fukushima

Contribution from the Department of Chemistry, Gunma University, Kiryu, Gunma 376, Japan.  
Received February 7, 1985

**Abstract:** Laser flash photolyses at 337 nm have been carried out on methanol solutions of the 1-naphthol and benzophenone system. It is found that hydrogen atom transfer reaction from the triplet 1-naphthol  ${}^3\text{ROH}^*$  (produced by triplet sensitization of benzophenone) to the ground benzophenone BP occurs effectively through the triplet complex  ${}^3\text{ROH}^*\cdots\text{OC}$  to give the 1-naphthoxy radical  $\text{RO}\cdot$  and the ketyl radical  $>\dot{\text{C}}\text{OH}$ . The triplet-triplet energy transfer  $k_{\text{ET}}$  ( $4.1 \times 10^9 \text{ M}^{-1} \text{ s}^{-1}$ ) from  ${}^3\text{BP}^*$  to ROH is competitive with both the usual hydrogen atom abstraction  $k_{\text{HA}}$  ( $7.4 \times 10^8 \text{ M}^{-1} \text{ s}^{-1}$ ) of  ${}^3\text{BP}^*$  from ROH and the quenching  $k_q'$  ( $2.2 \times 10^9 \text{ M}^{-1} \text{ s}^{-1}$ ) of  ${}^3\text{BP}^*$  induced by ROH at 290 K. These primary processes of  ${}^3\text{BP}^*$  are completed in 300 ns, and the equilibrium  ${}^3\text{ROH}^* + >\text{CO} \rightleftharpoons {}^3\text{ROH}^*\cdots\text{OC}$  is established very quickly. The equilibrium constant  $K^*$  for the  ${}^3\text{ROH}^*\cdots\text{OC}$  formation was obtained to be  $16.7 \text{ M}^{-1}$  at 290 K ( $\Delta H^* = -2.4 \text{ kcal mol}^{-1}$  and  $\Delta S^* = -2.7 \text{ eu}$ ). Then, the hydrogen atom transfer reaction takes place via the triplet complex with the rate constant  $k_{\text{HT}}$  ( $1.3 \times 10^6 \text{ s}^{-1}$  at 290 K,  $A_{\text{HT}} = 3.7 \times 10^9 \text{ s}^{-1}$ ;  $\Delta E_{\text{HT}} = 4.6 \text{ kcal mol}^{-1}$ ). Both  $\text{RO}\cdot$  and  $>\dot{\text{C}}\text{OH}$  produced by laser flash photolysis decay mainly via the radical reaction  $k_{\text{R}}$  between them with the rate constant  $1.7 \times 10^9 \text{ M}^{-1} \text{ s}^{-1}$  at 290 K. The reaction mechanism on the hydrogen atom transfer reaction from  ${}^3\text{ROH}^*$  (produced by triplet sensitization of BP) to yield  $\text{RO}\cdot$  and  $>\dot{\text{C}}\text{OH}$  is shown in detail.

Hydrogen atom transfer reactions of the triplet state of carbonyl compounds from a variety of substrates such as alcohols, hydrocarbons, and amines are well-known. The reaction proceeds by either hydrogen atom transfer or electron transfer followed by proton transfer. A large number of studies on intermolecular and intramolecular hydrogen-abstraction reactions of carbonyl triplets have been reported.<sup>2-12</sup> As for the photochemical features in the presence of phenols, reversible hydrogen abstraction by carbonyl triplets from phenols resulting in effective quenching of carbonyl triplets has been shown by Turro et al.<sup>13,14</sup> and Becker.<sup>15</sup>

CIDNP studies have demonstrated by ketyl radical formation during the photolysis of acetophenone-phenol mixtures.<sup>16,17</sup> A laser flash photolysis study of the quenching of carbonyl triplets by phenols has been reported by Das et al.<sup>18</sup> showing that the quenching of aromatic carbonyl triplets by phenols is a very fast process for both  $n,\pi^*$  and  $\pi,\pi^*$  states.

However, little attention has been paid to hydrogen atom transfer from triplet aromatic compounds to the ground state of the aromatic carbonyl compounds until very recently. In a preliminary report,<sup>19</sup> we have demonstrated the hydrogen atom transfer reaction from triplet 2-naphthylammonium ion to ground benzophenone (or acetophenone) in a laser flash photolysis study, while in the excited singlet state of the ammonium ion proton transfer takes place effectively.<sup>20</sup>

In the present paper, we report the hydrogen atom transfer reaction from triplet naphthol (produced by triplet sensitization of benzophenone) to ground benzophenone by means of laser flash photolysis.

### Experimental Section

**Materials.** Benzophenone and acetophenone used were the same as those reported elsewhere.<sup>21</sup> 1-Naphthol (G.R. grade, Wako) was purified by two recrystallizations from ethanol-water (1:1) mixtures. Methanol (Spectrosol, Wako) was used as a solvent.

(1) This work was supported by a Scientific Research Grant-in Aid of the Ministry of Education of Japan (No. 58470001 and 58340028). A part of the work was presented at the Symposium on Molecular Structures, Nagoya, October, 1984.

(2) Scaiano, J. C. *J. Photochem.* **1973/1974**, *2*, 81.

(3) Wagner, P. J.; Hammond, G. S. *Adv. Photochem.* **1968**, *5*, 21.

(4) Wagner, P. J. *Acc. Chem. Res.* **1971**, *4*, 168.

(5) Wagner, P. J. *Top. Current Chem.* **1976**, *66*, 1.

(6) Turro, N. J.; Dalton, J. C.; Dawes, K.; Farrington, G.; Hautala, R.; Morton, D.; Niemczyk, M.; Schore, N. *Acc. Chem. Res.* **1972**, *5*, 92.

(7) Dalton, J. C.; Turro, N. J. *Annu. Rev. Phys. Chem.* **1970**, *21*, 499.

(8) Turro, N. J. "Modern Molecular Photochemistry"; Benjamin/Cummings: Menlo Park, 1978.

(9) Cohen, S. G.; Parola, A.; Parsons, G. H., Jr. *Chem. Rev.* **1973**, *73*, 141.

(10) (a) Formosinho, S. J. *J. Chem. Soc., Faraday Trans. 2* **1976**, *72*, 1913. (b) Formosinho, S. J. *J. Chem. Soc., Faraday Trans. 2* **1978**, *74*, 1978.

(11) Okada, T.; Tashita, N.; Mataga, N. *Chem. Phys. Lett.* **1980**, *75*, 220.

(12) Okada, T.; Karaki, T.; Mataga, N. *J. Am. Chem. Soc.* **1982**, *104*, 7191.

(13) Peters, K. S.; Freilich, S. C.; Shaefer, C. G. *J. Am. Chem. Soc.* **1980**, *102*, 5701.

(14) Shaefer, G. G.; Peters, K. S. *J. Am. Chem. Soc.* **1980**, *102*, 5766.

(15) Simon, J. D.; Peters, K. S. *J. Am. Chem. Soc.* **1981**, *103*, 6403.

(16) Turro, N. J.; Engel, R. *J. Am. Chem. Soc.* **1981**, *103*, 6403; *Mol. Photochem.* **1969**, *1*, 143, 235.

(17) Turro, N. J.; Lee, T. *J. Mol. Photochem.* **1970**, *2*, 185.

(18) Becker, H. D. *J. Org. Chem.* **1967**, *32*, 211, 2124, 2140.

(16) Rosenfeld, S. M.; Lawler, R. G.; Ward, H. R. *J. Am. Chem. Soc.* **1973**, *95*, 946. Maurer, H. M.; Gardini, G. P.; Bargon, J. *J. Chem. Soc., Chem. Commun.* **1979**, 272.

(17) Deboer, J. W. M.; Hutchinson, D. A.; Hawly, R.; Wan, J. K. S. *Chem. Phys.* **1979**, *43*, 81.

(18) Das, P. K.; Encinas, M. V.; Scaiano, J. C. *J. Am. Chem. Soc.* **1981**, *103*, 4154.

(19) Shizuka, H.; Fukushima, M. *Chem. Phys. Lett.* **1983**, *101*, 598.

(20) Tsutsumi, K.; Shizuka, H. *Chem. Phys. Lett.* **1977**, *52*, 485; *Z. Phys. Chem. (Wiesbaden)* **1978**, *111*, 129. Shizuka, H. *Acc. Chem. Res.* **1985**, *18*, 141.

(21) Shizuka, H.; Kimura, E. *Can. J. Chem.* **1984**, *62*, 2041.

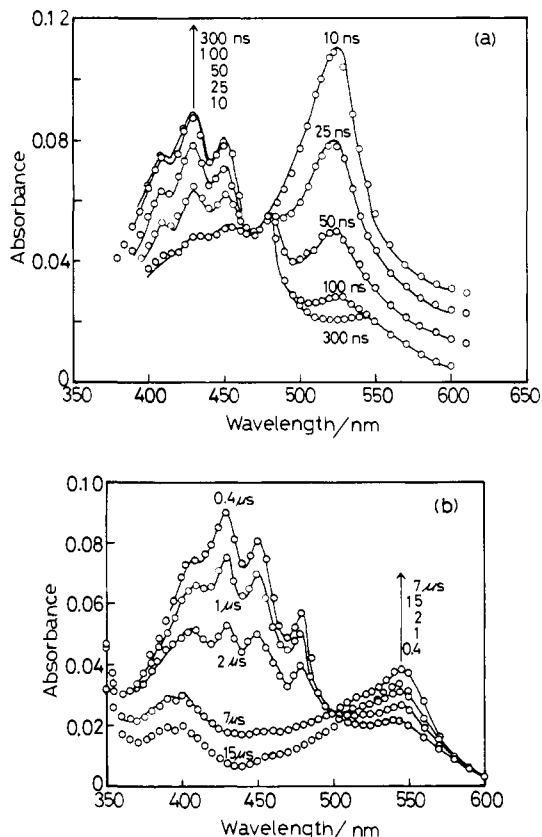


**Figure 1.** (a) Nanosecond time-resolved transient absorption spectra of benzophenone ( $6.67 \times 10^{-3}$  M) in the presence of 1-naphthol ( $3.0 \times 10^{-3}$  M) in methanol at 290 K, obtained by laser flash photolysis at 337 nm. Circle: observed; solid curve: calculated. For details see text. (b) Transient absorption spectra on the  $\mu$ s time scale for the benzophenone ( $6.67 \times 10^{-3}$  M) and 1-naphthol ( $3.0 \times 10^{-3}$  M) system at 290 K, obtained by laser flash photolysis at 337 nm. Circle: observed; solid curve: calculated. For details see text.

**Sample Preparations.** The concentrations of 1-naphthol were used in the range of  $1-5 \times 10^{-3}$  M (usually  $3.0 \times 10^{-3}$  M), and for benzophenone  $0.13-1.3 \times 10^{-2}$  M. All sample solutions in a 10-mm path length were thoroughly degassed by means of freeze-pump-thaw cycles on a high vacuum line. Spectral data regarding transients were obtained by a fresh sample to avoid excessive exposure to the laser pulse.

**Laser Flash Photolysis Instrument.** A nanosecond  $N_2$  laser system at 337 nm (Japan Dynamic JS-1000L; pulse width 5 ns; laser power 5 mJ) was used for sample excitation. The monitoring system consisted of a pulsed UXL-150D xenon lamp. A MC-20N monochromator (Rittu) and a HTV R928 photomultiplier tube were used for the detection part. The transient signal was recorded with a transient memory (Kawasaki Electronics, MR-50E), a 100-MHz storage oscilloscope (Iwatsu TS-8123), or a 200 MHz oscilloscope (Iwatsu SS-6200).

## Results

**Laser Flash Photolysis of Benzophenone in the Presence of 1-Naphthol.** Figure 1 shows the time-resolved transient absorption spectra of benzophenone ( $6.67 \times 10^{-3}$  M) in the presence of 1-naphthol ( $3.0 \times 10^{-3}$  M) in methanol at 290 K, obtained by nanosecond laser flash photolysis at 337 nm. The transient spectra on the nanosecond time scale have two band maxima, and the 525-nm band decrease accompanies an increase of the 430-nm band. Moreover, one can clearly observe the existence of an isosbestic point at 480 nm. It is obvious that the 525-nm band corresponds to the  $T_n \leftarrow T_1$  absorption band of benzophenone (BP).<sup>22,23</sup> The 430-nm band with vibrational structures was very similar to the  $T_n \leftarrow T_1$  absorption spectrum ( $\lambda_{\max} = 435$  nm) of 1-methoxynaphthalene and it was quenched markedly by dissolved oxygen. The shorter wavelength band is, therefore, ascribed to

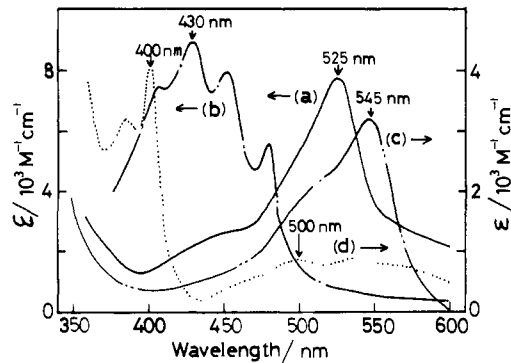


**Figure 2.** Absorption spectra of transient species obtained by laser flash photolysis at 337 nm: (a) the  $T_n \leftarrow T_1$  absorption spectrum of BP in methanol, (b) the  $T_n \leftarrow T_1$  absorption spectrum of ROH in methanol, (c) the absorption spectrum of  $>\dot{C}OH$  in methanol, and (d) the absorption spectrum of  $RO\cdot$  in methanol. For details see text.

the  $T_n \leftarrow T_1$  absorption spectrum of 1-naphthol. The spectral change in Figure 1a shows that 1-naphthol triplet ( ${}^3ROH^*$ ) is produced by triplet sensitization of BP. The triplet energies of BP and ROH are known to be 69.2 and 58.6 kcal mol<sup>-1</sup> in polar media.<sup>24</sup> At the nanosecond region, the fluorescence emission at shorter wavelength was observed due to the direct excitation of 1-naphthol (ROH) by a laser pulse at 337 nm. However, the ratio of the direct excitation of ROH ( $3.0 \times 10^{-3}$  M) to that of BP ( $6.67 \times 10^{-3}$  M) was less than 1%, judging from the absorbance of ROH at 337 nm. Therefore, it can be said that the direct excitation of ROH is an extremely minor process in the present laser flash photolysis experiments. Little spectral change between the delay times 300 and 400 ns from the start of laser pulsing was observed as shown in parts a and b of Figure 1, respectively. This result suggests that the triplet-triplet energy transfer from  ${}^3BP^*$  to ROH was established by the delay time ( $t$ ) of 300 ns. The transient absorption spectra at  $t = 300$  and 400 ns have two band maxima at 430 and 545 nm; the former band is due to the  $T_n \leftarrow T_1$  absorption of ROH as described above and the latter one is ascribed to both the benzophenone ketyl radical ( $>\dot{C}OH$ )<sup>23</sup> and 1-naphthoxy radical ( $RO\cdot$ )<sup>25</sup> by comparison with their reference spectra (see Figure 2). The usual hydrogen atom abstraction reactions of  ${}^3BP^*$  from solvent molecules<sup>2,5,7,8,10</sup> or from phenols<sup>13-15,18</sup> are well-known.

From the spectral analyses of Figure 1a using the molar extinction coefficients  $\epsilon$  of the transient species  ${}^3BP^*$ ,  ${}^3ROH^*$ ,  $>\dot{C}OH$ , and  $RO\cdot$  (see Table I and Figure 2), their concentrations produced by laser flash photolysis can be determined as follows. The concentration of  ${}^3BP^*$  produced via fast intersystem crossing<sup>8,26-28</sup> of the excited singlet state of benzophenone ( ${}^1BP^*$ ) by single laser pulse excitation was ca.  $1.6 \times 10^{-5}$  M using  $\epsilon = 7800$  M<sup>-1</sup> cm<sup>-1</sup> at 525 nm in methanol. For  ${}^3ROH^*$  produced by triplet sensitization by  ${}^3BP^*$ , its concentration was obtained to be  $9.3 \times 10^{-6}$  M at  $t = 0.3-0.4$   $\mu$ s, using  $\epsilon = 9000$  M<sup>-1</sup> cm<sup>-1</sup> at 430 nm in methanol. The results show that the triplet-triplet energy transfer efficiency  $\phi_{ET}$  is equal to 0.58 ( $\pm 0.11$ ). The concentrations of  $>\dot{C}OH$  and  $RO\cdot$  produced by the usual hydrogen atom abstraction (HA) reactions of  ${}^3BP^*$  were determined to be  $4.2 \times 10^{-6}$  and  $1.7 \times 10^{-6}$  M, respectively, by single laser pulse excitation. The difference ( $2.5 \times 10^{-6}$  M) between the concentrations of  $>\dot{C}OH$  and  $RO\cdot$  corresponds to the  $>\dot{C}OH$  concentration produced by the usual HA reaction of  ${}^3BP^*$  from solvent

(24) Murov, S. L. "Handbook of Photochemistry"; Marcel Dekker: New York, 1973.

(25) Das, P. K.; Encinas, M. V.; Scaiano, J. C. *J. Am. Chem. Soc.* **1981**, *103*, 4162.

(26) El-Sayed, M. A. *J. Chem. Phys.* **1962**, *36*, 573; **1963**, *38*, 2834; **1964**, *41*, 2462.

(27) Damschen, D. E.; Merritt, C. D.; Perry, D. L.; Scott, G. W.; Talley, L. D. *J. Phys. Chem.* **1978**, *82*, 2268.

(28) Anderson, R. W., Jr.; Hockstrasser, R. M.; Lutz, H.; Scott, G. W. *J. Chem. Phys.* **1974**, *61*, 2500. Anderson, R. W., Jr.; Hockstrasser, R. M.; Lutz, H.; Scott, G. W. *Chem. Phys. Lett.* **1978**, *28*, 153.

(22) Ledger, M. B.; Porter, G. *J. Chem. Soc., Faraday Trans. 1* **1972**, *68*, 539.

(23) Land, E. *J. Proc. R. Soc. London* **1968**, *A305*, 457.

(methanol) molecules, since the concentration ( $1.7 \times 10^{-6}$  M) of RO $\cdot$  should be the same as that of  $>\dot{\text{C}}\text{OH}$  produced by the HA reaction of  ${}^3\text{BP}^*$  from ROH. The efficiency  $\phi_{\text{HA}'}$  for the HA reaction of  ${}^3\text{BP}^*$  from ROH to produce  $>\dot{\text{C}}\text{OH}$  or RO $\cdot$  is estimated to be 0.11. Therefore, the transient spectrum at  $t = 0.3\text{--}0.4$   $\mu\text{s}$  in Figure 1a,b consists of additive absorbances of  ${}^3\text{ROH}^*$  ( $9.3 \times 10^{-6}$  M),  $>\dot{\text{C}}\text{OH}$  ( $4.2 \times 10^{-6}$  M), and RO $\cdot$  ( $1.7 \times 10^{-6}$  M). The spectrum calculated agreed fairly well with that obtained experimentally within 10% error.

The absorbance at 545 nm ( $>\dot{\text{C}}\text{OH}$  and RO $\cdot$ ) increased with a decrease in that at 430 nm ( ${}^3\text{ROH}^*$ ) in the range of 0.4–7  $\mu\text{s}$ , as shown in Figure 1b. The spectral change on the  $\mu\text{s}$  time scale is accompanied with an isosbestic point at 500 nm. This finding indicates that hydrogen atom transfer (HT) occurs effectively from  ${}^3\text{ROH}^*$  to the ground state of BP to produce  $>\dot{\text{C}}\text{OH}$  and RO $\cdot$ . A new peak at near 400 nm appears at  $t = 7\text{--}15$   $\mu\text{s}$  after complete decay of  ${}^3\text{ROH}^*$ , which is ascribed to the absorption due to RO $\cdot$ <sup>25</sup> by comparison with the reference spectrum of RO $\cdot$  (see Figure 2). The concentration of  $>\dot{\text{C}}\text{OH}$  or RO $\cdot$  produced by the HT reaction from  ${}^3\text{ROH}^*$  to the ground BP by single laser pulse excitation was determined to be  $4.4 \times 10^{-6}$  M from the absorbance at 545 nm in Figure 1b with use of the corresponding  $\epsilon$  values [ $(\epsilon_{>\dot{\text{C}}\text{OH}})_{545} = 3220 \text{ M}^{-1} \text{ cm}^{-1}$ ;<sup>23</sup>  $(\epsilon_{\text{RO}\cdot})_{545} = 830 \text{ M}^{-1} \text{ cm}^{-1}$ , see Table I]. Therefore, the reaction quantum yield  $\Phi_{\text{HT}}$  for the BP ( $6.67 \times 10^{-3}$  M) and ROH ( $3.0 \times 10^{-3}$  M) system at 337 nm at 290 K can be obtained to be ca. 0.28 ( $\pm 0.05$ ) ( $\Phi_{\text{HT}} = 4.4 \times 10^{-6} \text{ M}/[{}^3\text{BP}^*]_{\text{max}} = 4.4 \times 10^{-6} \text{ M}/1.6 \times 10^{-5} \text{ M}$ ). The HT efficiency  $\phi_{\text{HT}}$  from  ${}^3\text{ROH}^*$  to BP to produce  $>\dot{\text{C}}\text{OH}$  and RO $\cdot$  is also determined to be 0.48 ( $\pm 0.09$ ) ( $\phi_{\text{HT}} = \Phi_{\text{HT}}/\phi_{\text{ET}} = 0.28/0.58$  or  $\phi_{\text{HT}} = 4.4 \times 10^{-6} \text{ M}/[{}^3\text{ROH}^*]_{\text{max}} = 4.4 \times 10^{-6}/9.3 \times 10^{-6}$ ). A similar HT reaction from the triplet naphthyl ammonium ion to the ground BP has been demonstrated recently by this laboratory.<sup>19</sup>

**Reference Absorption Spectra of Benzophenone Triplet, 1-Naphthol Triplet, Ketyl Radical, and Naphthoxy Radical.** The transient absorption spectra of the intermediates ( ${}^3\text{BP}^*$ ,  ${}^3\text{ROH}^*$ ,  $>\dot{\text{C}}\text{OH}$ , and RO $\cdot$ ) produced by nanosecond laser flash photolysis are shown in parts a–d of Figure 2, respectively. The  $T_n \leftarrow T_1$  absorption spectrum of BP was obtained by nanosecond laser flash photolysis of BP ( $6.67 \times 10^{-3}$  M in methanol) in the presence of ROH at the delay time 25 ns. The transient spectrum with  $\lambda_{\text{max}} = 525$  nm is well-known. The molar extinction coefficient  $\epsilon$  of  ${}^3\text{BP}^*$  was estimated to be  $7800 \text{ M}^{-1} \text{ cm}^{-1}$  at 525 nm in methanol by comparing the  $T_n \leftarrow T_1$  absorption spectra of BP in both benzene and methanol on the assumption that the oscillator strength for the absorption band at 525 nm is the same as that (0.0795) in benzene ( $\epsilon = 7400 \text{ M}^{-1} \text{ cm}^{-1}$  at 532.5 nm in benzene).<sup>29</sup> The  $T_n \leftarrow T_1$  absorption spectrum of ROH in methanol was measured by sensitization of ROH by triplet acetophenone upon laser excitation at 337 nm. In the case of acetophenone the HT reaction from  ${}^3\text{ROH}^*$  to the ground acetophenone occurred to a small extent in the  $\mu\text{s}$  region. However, the usual HA reaction from solvent molecules (or from ROH) took place scarcely in the early stage of the delay times less than 0.4  $\mu\text{s}$  in contrast to the case of BP. This reason is due to the difference in electronic structures between them; i.e.,  ${}^3\text{BP}^*$  is  ${}^3(n,\pi^*)$ , but acetophenone in polar media is  ${}^3(\pi,\pi^*)$ .<sup>30</sup> The  $\epsilon$  value of  ${}^3\text{ROH}^*$  at 430 nm was determined to be  $9000 \text{ M}^{-1} \text{ cm}^{-1}$  in methanol by comparison with the  $T_n \leftarrow T_1$  absorption intensities of  ${}^3\text{ROH}^*$  at 430 nm in methanol and of naphthalene triplet at 415 nm in cyclohexane obtained by triplet sensitization by acetophenone upon laser pulse excitation at 337 nm. The  $\epsilon$  value of naphthalene is known to be  $24500 \text{ M}^{-1} \text{ cm}^{-1}$ <sup>29</sup> at 415 nm in cyclohexane. The absorption spectrum of the benzophenone ketyl radical ( $>\dot{\text{C}}\text{OH}$ ) was obtained by laser flash photolysis of BP ( $6.67 \times 10^{-3}$  M in methanol) at the delay time = 20  $\mu\text{s}$ , whose spectrum is well-known (the value of  $3220 \text{ M}^{-1} \text{ cm}^{-1}$ <sup>23</sup> was used as the  $\epsilon$  value of  $>\dot{\text{C}}\text{OH}$  at 545 nm). The absorption spectrum of RO $\cdot$  was obtained by laser flash photolysis of a di-*tert*-butyl peroxide–benzene mixture (2:1 in volume) in the presence of 1-naphthol ( $3.0 \times 10^{-3}$  M). The transient spectra at  $t = 2$   $\mu\text{s}$  has two band maxima at 392 and

**Table I.** Molar Extinction Coefficients  $\epsilon$  for Transient Species Produced by Laser Flash Photolysis

$\lambda$ , nm	$\epsilon$ , $\text{M}^{-1} \text{ cm}^{-1}$				
	${}^3\text{BP}^*$ <sup>a</sup>	${}^3\text{ROH}^*$ <sup>a</sup>	$>\dot{\text{C}}\text{OH}$ <sup>a</sup>	RO $\cdot$ <sup>a</sup>	RO $\cdot$ <sup>b</sup>
430	2190	9000	610	200	220
525	7800 <sup>d</sup>	750	2460	820	810
545	3820	570	3220	830	830
560	3010	510	2070	790	820

<sup>a</sup>In methanol. <sup>b</sup>In benzene. For details see text. <sup>c</sup>Taken from ref 23. <sup>d</sup>The  $\epsilon$  values for the  $T_n \leftarrow T_1$  absorption band at 532.5 nm in benzene have been reported; 7400 in ref 29 and 7100 ( $\pm 800$ ) in ref 18.

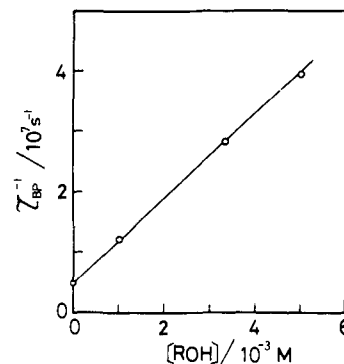


**Figure 3.** The Stern–Volmer plot of the triplet decay rate at BP ( $\tau_{\text{BP}}^{-1}$ ) as a function of  $[\text{ROH}]$  at 290 K. See text.

500 nm in benzene. The peak of RO $\cdot$  at 392 nm is entirely the same as that reported by Scaiano's group.<sup>25</sup> The estimation of the  $\epsilon$  values of RO $\cdot$  was made by analyzing the time traces of the absorbances at both 545 and 560 nm in the laser flash photolysis experiment of BP ( $6.67 \times 10^{-3}$  M) with ROH ( $3.0 \times 10^{-3}$  M) in methanol,<sup>31</sup> using the absorbance ratio ( $A_{560}/A_{545} = 0.98$ ) of RO $\cdot$ . Here  $A_{560}$  and  $A_{545}$  denote the absorbance at 560 and 545 nm, respectively, in Figure 2. In this estimation we assumed that little spectral change in solvents between benzene and methanol is present in the broad 500-nm band of RO $\cdot$ . The absorption spectrum of RO $\cdot$  in methanol can be obtained by spectral fitting based on the spectral change in Figure 1b. The  $\epsilon$  values of RO $\cdot$  at 545 and 400 nm were determined to be 830 and  $4020 \text{ M}^{-1} \text{ cm}^{-1}$  within 10% errors, respectively. The values of the transient species produced in the laser flash photolysis are listed in Table I.

**Quenching of  ${}^3\text{BP}^*$  by ROH in Methanol.** The quenching experiments of  ${}^3\text{BP}^*$  by ROH have been carried out by means of nanosecond laser flash photolysis of BP in methanol at 290 K. The decay rate of  ${}^3\text{BP}^*$  monitored at 525 nm decreased significantly with increasing the concentration of ROH. The transient peak at 525 nm of  ${}^3\text{BP}^*$  decayed with single exponential function. Figure 3 shows the plot of the decay rate  $\tau_{\text{BP}}^{-1}$  of  ${}^3\text{BP}^*$  as a function of the concentration of ROH. The quenching rate constant  $k_q$  was obtained to be  $7.0 \times 10^9 \text{ M}^{-1} \text{ s}^{-1}$  in methanol at 290 K from the slope of the straight line in Figure 3. The lifetime of  ${}^3\text{BP}^*$  ( $\tau_{\text{BP}}^0$ ) in methanol at 290 K in the absence of ROH was 0.20  $\mu\text{s}$ . This value is the same as that of the lifetime of  ${}^3\text{BP}^*$  obtained from the intercept from the line in Figure 3. The  $k_q$  value involves the rate constants for the triplet–triplet energy transfer  $k_{\text{ET}}$  from  ${}^3\text{BP}^*$  to ROH, the hydrogen atom abstraction  $k_{\text{HA}'}$  of  ${}^3\text{BP}^*$  from ROH, and the nonradiative quenching of  $k_q'$  of  ${}^3\text{BP}^*$  induced by ROH.

(30) Lammola, A. A. *J. Chem. Phys.* **1967**, *47*, 4810.

(31) The estimation of the  $\epsilon$  values of RO $\cdot$  at 545 nm was made as follows:  $\Delta A_{545} = \{(\epsilon_{>\dot{\text{C}}\text{OH}})_{545} + (\epsilon_{\text{RO}\cdot})_{545}\} \Delta C$  and  $\Delta A_{560} = \{(\epsilon_{>\dot{\text{C}}\text{OH}})_{560} + (\epsilon_{\text{RO}\cdot})_{560}\} \Delta C$ , where  $\Delta A_{545}$  and  $\Delta A_{560}$  denote the net absorbance increases ( $1.7 \times 10^{-2}$  and  $9.03 \times 10^{-3}$  at 545 and 560 nm respectively) between the delay times 0.8 and 1.8  $\mu\text{s}$ ,  $\epsilon$  the corresponding molar extinction coefficients at 545 and 560 nm [the values of  $(\epsilon_{>\dot{\text{C}}\text{OH}})_{545}$  and  $(\epsilon_{>\dot{\text{C}}\text{OH}})_{560}$  are known to be 3220<sup>23</sup> and 2070, respectively], the ratio of  $(\epsilon_{\text{RO}\cdot})_{560}/(\epsilon_{\text{RO}\cdot})_{545}$  is 0.98, and  $\Delta C$  is the increase in the concentration of  $>\dot{\text{C}}\text{OH}$  (or RO $\cdot$ ) between 0.8 and 1.8  $\mu\text{s}$ . From the above equations, the values of the  $(\epsilon_{\text{RO}\cdot})_{545}$  and  $(\epsilon_{\text{RO}\cdot})_{560}$  were determined to be 830 and  $820 \text{ M}^{-1} \text{ cm}^{-1}$ , respectively.

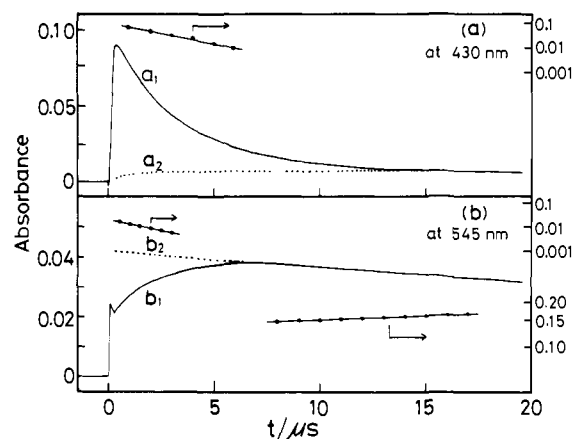


**Figure 4.** Time traces of absorbances  $a_1$  and  $b_1$  monitored at 430 nm (a) and 545 nm (b), respectively, on the  $\mu\text{s}$  time scale for the BP ( $6.67 \times 10^{-3}$  M) and ROH ( $3.0 \times 10^{-3}$  M) system in methanol at 290 K obtained by laser flash photolysis. Curve  $a_2$  is the rise curve of RO $\cdot$  and  $>\dot{\text{C}}\text{OH}$  at 430 nm and curve  $b_2$  the extrapolation of decay in curve  $b_1$  at 545 nm.  $\log \{\text{curve } a_1 - \text{curve } a_2\}$  vs.  $t$  and  $\log \{\text{curve } b_2 - \text{curve } b_1\}$  vs.  $t$  are plotted in parts a and b, respectively. Both RO $\cdot$  and  $>\dot{\text{C}}\text{OH}$  decay according to the second-order kinetics:  $[2.303 / \{[>\dot{\text{C}}\text{OH}]_{\text{max}} - [\text{RO}\cdot]_{\text{max}}\}] \log \{[>\dot{\text{C}}\text{OH}]_t / [\text{RO}\cdot]_t\} = k_{\text{R}}t + \text{constant}$ , where  $[>\dot{\text{C}}\text{OH}]_t$  and  $[\text{RO}\cdot]_t$  represent the concentrations of  $>\dot{\text{C}}\text{OH}$  and RO $\cdot$  at  $t$ . The plot of  $\log \{[>\dot{\text{C}}\text{OH}]_t / [\text{RO}\cdot]_t\}$  vs.  $t$  gives a straight line. For details see text.

**Table II.** The Observed Decay Constants ( $\tau_{\text{obsd}}^{-1}$ ) of  ${}^3\text{ROH}^*$  Monitored at 430 nm in Methanol<sup>a</sup>

[>CO], 10 <sup>-2</sup> M	$\tau_{\text{obsd}}^{-1}, 10^5 \text{ s}^{-1}$					
	274 K <sup>b</sup>	280 K <sup>b</sup>	290 K <sup>b</sup>	300 K <sup>b</sup>	310 K <sup>b</sup>	320 K <sup>b</sup>
0.13 <sub>3</sub>	1.4 <sub>8</sub>	1.5 <sub>9</sub>	1.7	1.8 <sub>1</sub>	1.9 <sub>6</sub>	2.1 <sub>5</sub>
0.27	1.6 <sub>9</sub>	1.8 <sub>4</sub>	1.9 <sub>9</sub>	2.1 <sub>3</sub>	2.3 <sub>6</sub>	2.6 <sub>2</sub>
0.40	1.9	2.0 <sub>8</sub>	2.2 <sub>6</sub>	2.4 <sub>4</sub>	2.7 <sub>4</sub>	3.0 <sub>6</sub>
0.53	2.0 <sub>9</sub>	2.3 <sub>1</sub>	2.5 <sub>2</sub>	2.7 <sub>3</sub>	3.1 <sub>2</sub>	3.5
0.66 <sub>7</sub>	2.2 <sub>8</sub>	2.5 <sub>2</sub>	2.7 <sub>8</sub>	3.0 <sub>2</sub>	3.4 <sub>8</sub>	3.9 <sub>2</sub>
0.83	2.5	2.7 <sub>8</sub>	3.0 <sub>8</sub>	3.3 <sub>6</sub>	3.9 <sub>1</sub>	4.4 <sub>3</sub>
1.0	2.7 <sub>1</sub>	3.0 <sub>3</sub>	3.3 <sub>7</sub>	3.6 <sub>9</sub>	4.3 <sub>3</sub>	4.9 <sub>3</sub>
1.3 <sub>3</sub>	3.0 <sub>8</sub>	3.4 <sub>8</sub>	3.9 <sub>1</sub>	4.3 <sub>0</sub>	5.1 <sub>2</sub>	5.8 <sub>7</sub>

<sup>a</sup> Errors within 5%. <sup>b</sup> Temperature was controlled within  $\pm 0.5$  K.

#### Hydrogen Atom Transfer Reactions under Various Conditions.

Figure 4 shows the time traces  $a_1$  and  $b_1$  of absorbances on the  $\mu\text{s}$  time scale, obtained by laser flash photolysis of BP ( $6.67 \times 10^{-3}$  M) in methanol in the presence of ROH ( $3.0 \times 10^{-3}$  M) at 290 K monitored at 430 nm (a) and 545 nm (b), respectively. The plot of  $\log \{\text{curve } a_1 - \text{curve } a_2\}$  vs. the delay time  $t$  gives a straight line in the early stage of the reaction ( $t \leq 6.0 \mu\text{s}$ ), where curve  $a_2$  is the absorbances of RO $\cdot$  and  $>\dot{\text{C}}\text{OH}$  at 430 nm produced by the HT reaction and it can be estimated from the time trace  $b_1$  at 545 nm for the formation of RO $\cdot$  and  $>\dot{\text{C}}\text{OH}$ . That is, the value of curve  $a_1$  minus curve  $a_2$  corresponds to the net absorbance of  ${}^3\text{ROH}^*$  at 430 nm. The decay rate of  ${}^3\text{ROH}^*$  is obtained to be  $2.7_8 \times 10^5 \text{ s}^{-1}$  from the slope in Figure 4a. On the other hand, the rise rate at 545 nm ( $>\dot{\text{C}}\text{OH}$  and RO $\cdot$ ) can be determined from the straight line of the plot of  $\log \{\text{curve } b_2 - b_1\}$  vs.  $t$  in Figure 4b, where curve  $b_2$  is estimated from the decay feature of the time trace of curve  $b_1$  for RO $\cdot$  and  $>\dot{\text{C}}\text{OH}$ . The results show that the 430-nm transient of  ${}^3\text{ROH}^*$  is a precursor of the 545-nm transients.

We measured the decay rates  $\tau_{\text{obsd}}^{-1}$  of  ${}^3\text{ROH}^*$ , i.e., the formation rates of  $>\dot{\text{C}}\text{OH}$  (or RO $\cdot$ ), under various temperatures and various concentrations of BP. The results are listed in Table II. The values of  $\tau_{\text{obsd}}^{-1}$  increase considerably with increasing temperatures and they increase straightly with the concentration of BP up to  $[\text{BP}] = 6 \times 10^{-3}$  M as shown in Figure 5. However, the  $\tau_{\text{obsd}}^{-1}$  values do not increase linearly at the concentrations of BP higher than  $6 \times 10^{-3}$  M at each temperature. That is, the plot of  $\tau_{\text{obsd}}^{-1}$  vs.  $[\text{BP}]$  has a negative curve. The time trace for the decay of the radicals RO $\cdot$  and  $>\dot{\text{C}}\text{OH}$  is shown in Figure 4b.

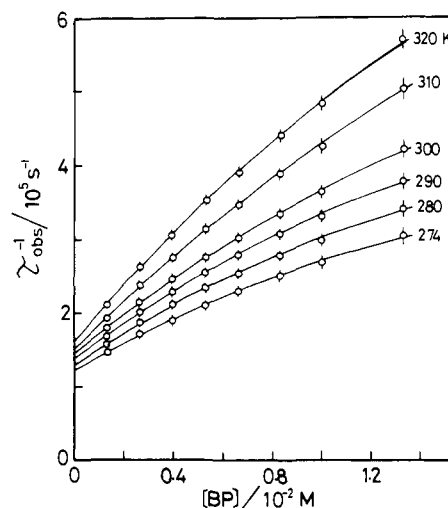
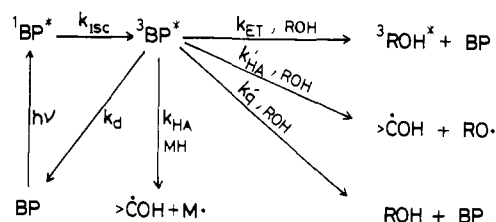


**Figure 5.** The decay rate ( $\tau_{\text{obsd}}^{-1}$ ) of  ${}^3\text{ROH}^*$  monitored at 430 nm as a function of  $[\text{BP}]$  at various temperatures. The solid curve denotes the calculated one from eq 9, which agrees well with the experimental data. See text.

#### Scheme I



The lifetime of  $>\dot{\text{C}}\text{OH}$  produced by laser flash photolysis of BP alone was very long (ca. ms), but the decay rate of  $>\dot{\text{C}}\text{OH}$  in the presence of RO $\cdot$  was not so slow, as can be seen in Figure 4b, suggesting occurrence of the reaction between RO $\cdot$  and  $>\dot{\text{C}}\text{OH}$ .

#### Discussion

**Primary Processes of Benzophenone Triplet in the Presence of 1-Naphthol: Triplet-Triplet Energy Transfer Quenching and Hydrogen Atom Abstraction Reactions.** On the basis of the experimental results, the primary processes of  ${}^3\text{BP}^*$  produced by fast intersystem crossing of  ${}^1\text{BP}^*$ ,<sup>26-28</sup> in the presence of ROH can be expressed by Scheme I, where  $k_d$  denotes the decay rate constant of  ${}^3\text{BP}^*$  [the  ${}^3(n, \pi^*)$  state of benzophenone] other than that of the decay caused by the HA reaction of  ${}^3\text{BP}^*$  from methanol in the absence of ROH,  $k_{\text{HA}}$  the rate constant for the usual HA reaction of  ${}^3\text{BP}^*$  from solvent (methanol:MH), and  $k_{\text{ET}}$ ,  $k_{\text{HA}'}$ , and  $k_q'$  the rate constants for the triplet-triplet energy transfer from  ${}^3\text{BP}^*$  to ROH, the HA reaction of  ${}^3\text{BP}^*$  from ROH, and the nonradiative quenching of  ${}^3\text{BP}^*$  induced by ROH, respectively. These reactions of  ${}^3\text{BP}^*$  in Scheme I are completed by  $t \sim 300$  ns as can be seen in Figure 1. The lifetime ( $\tau_{\text{BP}}^0$ ) of  ${}^3\text{BP}^*$  obtained is  $0.20 \mu\text{s}$  in the absence of ROH in methanol at 290 K, and therefore  $(\tau_{\text{BP}}^0)^{-1}$  is expressed as

$$(\tau_{\text{BP}}^0)^{-1} = k_d + k_{\text{HA}}[\text{MH}] = 5 \times 10^6 \text{ s}^{-1} \quad (1)$$

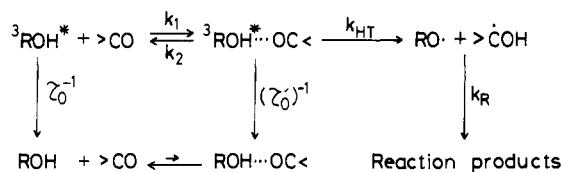
This value entirely agrees with that obtained by the intercept of the Stern-Volmer plot in Figure 3. From the quenching experiments of  ${}^3\text{BP}^*$  by ROH in Figure 3, it is shown that the value of  $k_q$  ( $7.0 \times 10^9 \text{ M}^{-1} \text{ s}^{-1}$ ) consists of  $k_{\text{ET}}$ ,  $k_{\text{HA}'}$ , and  $k_q'$ , as described above. Equation 2 is, therefore, obtained. The energy transfer

$$k_q = k_{\text{ET}} + k_{\text{HA}'} + k_q' = 7.0 \times 10^9 \text{ M}^{-1} \text{ s}^{-1} \quad (2)$$

efficiency  $\phi_{\text{ET}}$  obtained from the spectral analysis in Figure 1a is 0.58 in laser flash photolysis of BP ( $6.67 \times 10^{-3}$  M) in the presence of ROH ( $3.0 \times 10^{-3}$  M) in methanol at 290 K, as described above. From eq 2 and 3, the  $k_{\text{ET}}$  value can be evaluated

$$\phi_{\text{ET}} = k_{\text{ET}} / k_q = 0.58 \quad (3)$$

## Scheme II

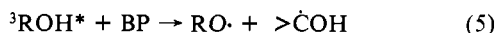


to be  $4.1 \times 10^9 \text{ M}^{-1} \text{ s}^{-1}$  at 290 K. Similarly, the  $k_{\text{HA}}'$  value is derived to be  $0.74 \times 10^9 \text{ M}^{-1} \text{ s}^{-1}$  from eq 2 and 4, using the HA reaction efficiency ( $\phi_{\text{HA}}' = 0.11$ ) of  ${}^3\text{BP}^*$  from ROH. Thus, the

$$\phi_{\text{HA}}' = k_{\text{HA}}'/k_q = 0.11 \quad (4)$$

value of the nonradiative quenching  $k_q'$  of  ${}^3\text{BP}^*$  induced by ROH is estimated to be  $2.2 \times 10^9 \text{ M}^{-1} \text{ s}^{-1}$  at 290 K, using eq 2 and the values of  $k_{\text{ET}}$  and  $k_{\text{HA}}'$ . That is, the efficiency  $\phi_q'$  for the  $k_q'$  process of  ${}^3\text{BP}^*$  is 0.31. It can be said that the reactions of  ${}^3\text{BP}^*$  with ROH are comprised of  $k_{\text{ET}}$  (58%),  $k_q'$  (31%), and  $k_{\text{HA}}'$  (11%) and that the  $k_{\text{ET}}$  value is 5.3 times greater than that of  $k_{\text{HA}}'$ . The value of  $k_{\text{HA}}'$  ( $0.74 \times 10^9 \text{ M}^{-1} \text{ s}^{-1}$ ) may be a reasonable value compared to those ( $\sim 10^9 \text{ M}^{-1} \text{ s}^{-1}$ ) of the hydrogen atom abstraction reaction of  ${}^3\text{BP}^*$  from phenols as reported by Scaiano's group.<sup>18</sup> The reason for the  $k_q'$  process induced by ROH is unknown exactly at the present stage. However, a possible explanation on  $k_q'$  is considered to be due to charge-transfer interaction between proton-donor (ROH) and -acceptor  $\pi$ -electron systems ( ${}^3\text{BP}^*$ ). Since  ${}^3\text{BP}^*$  has an intramolecular charge-transfer character from phenol groups to the carbonyl group to some extent in polar media on the basis of the acidity constants of aromatic ketones.<sup>21</sup> For the excited singlet state, it is well-known that hydrogen bonding interaction leads to the quenching of fluorescence, especially when two conjugate systems are directly combined by hydrogen bonding interaction.<sup>32-35</sup> It has been recently established by picosecond laser photolysis that the fluorescence quenching in conjugated  $\pi$ -electronic hydrogen bonding systems is caused by the formation of a nonfluorescent charge-transfer state in the excited hydrogen-bonded pair.<sup>32,33</sup> Anyway, the  $k_q'$  quenching process of  ${}^3\text{BP}^*$  induced by ROH is competitive with the energy transfer  $k_{\text{ET}}$  and hydrogen atom abstraction  $k_{\text{HA}}'$  processes. The primary process of  ${}^3\text{BP}^*$  in the present system is completed in ca. 300 ns at 290 K.

**Hydrogen Atom Transfer Reaction from Triplet 1-Naphthol to Ground Benzophenone.** After the triplet-triplet energy transfer reaction  $k_{\text{ET}}$  from  ${}^3\text{BP}^*$  to ROH in Scheme I, the hydrogen atom transfer (HT) reaction occurs effectively from  ${}^3\text{ROH}^*$  to the ground BP to produce the benzophenone ketyl radical  $>\dot{\text{C}}\text{OH}$  and the 1-naphthoxy radical  $\text{RO}\cdot$  as described above. However, this HT reaction does not take place directly, because the plot of  $\tau_{\text{obsd}}^{-1}$



(the decay rate of  ${}^3\text{ROH}^*$ , i.e., the rise rate for the product formation of  $>\dot{\text{C}}\text{OH}$  or  $\text{RO}\cdot$ ) as a function of [BP] shows a negative curve, as shown in Figure 5. A possibility of formation of a complex between BP and ROH in the ground state is unlikely under the experimental conditions, since the Stern-Volmer plot of the decay rate of  ${}^3\text{BP}^*$  vs. [ROH] gives a straight line as can be seen in Figure 3. The experimental results can be accounted for by Scheme II, where  $>\text{CO}$  denotes of the ground state of BP,  ${}^3\text{ROH}^*\cdots\text{OC} <$  the 1:1 triplet complex between  ${}^3\text{ROH}^*$  and  $\text{OC} <$ ,  $\text{ROH}\cdots\text{OC} <$  the 1:1 complex in the ground state,  $k_1$  and  $k_2$  the rate constants for association and dissociation between  ${}^3\text{ROH}^*$  and  $>\text{CO}$ , respectively,  $\tau_0$  and  $\tau_0'$  the lifetimes of  ${}^3\text{ROH}^*$  and the  ${}^3\text{ROH}^*\cdots\text{OC} <$  complex, respectively, and  $k_{\text{HT}}$  and  $k_{\text{R}}$  the rate

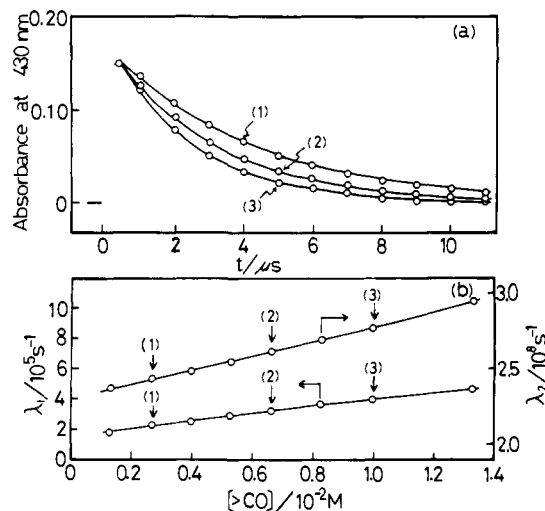


**Figure 6.** (a) The decay function  $F(t)$  of the 430-nm transient at 290 K at the concentration of  $>\text{CO}$ : (1)  $0.27 \times 10^{-2}$ , (2)  $0.667 \times 10^{-2}$ , and (3)  $1.0 \times 10^{-2} \text{ M}$ . Circle: observed; solid curve: calculated. (b) The decay parameters  $\lambda_1$  and  $\lambda_2$  fitted to  $F(t)$  as a function of  $[>\text{CO}]$ ; e.g., (1)  $\lambda_1 = 2.19 \times 10^5 \text{ s}^{-1}$ ,  $\lambda_2 = 2.44 \times 10^8 \text{ s}^{-1}$ ; (2)  $\lambda_1 = 3.23 \times 10^5 \text{ s}^{-1}$ ,  $\lambda_2 = 2.62 \times 10^8 \text{ s}^{-1}$ , and (3)  $\lambda_1 = 3.99 \times 10^5 \text{ s}^{-1}$ ,  $\lambda_2 = 2.77 \times 10^8 \text{ s}^{-1}$ .

constants for the hydrogen atom transfer reaction and the reaction between radicals, respectively. For the naphthylammonium ion ( $\text{RNH}_3^+$ )-BP system, it has been found very recently that the hydrogen atom transfer from  ${}^3\text{RNH}_3^{*+}$  to BP occurs similarly via the triplet complex  ${}^3\text{RNH}_3^{*+}\cdots\text{OC} <$  to produce the cation radical  $\text{RNH}_2^{\cdot+}$  and the ketyl radical  $>\dot{\text{C}}\text{OH}$ .<sup>36</sup> There was no spectral change in the  $T_n \leftarrow T_1$  transient absorptions between  ${}^3\text{RNH}_3^{*+}$  and  ${}^3\text{RNH}_3^{*+}\cdots\text{OC} <$ . In the present systems, little spectral change in the  $T_n \leftarrow T_1$  absorptions between free  ${}^3\text{ROH}^*$  and  ${}^3\text{ROH}^*\cdots\text{OC} <$  was observed. The observation suggests that the triplet complex is a locally excited triplet state, in which the electronic structure of the complex is close to that of free  ${}^3\text{ROH}^*$ . This suggestion may be reasonable since there is little or no  $\pi$ -conjugation between  ${}^3\text{ROH}^*$  and  $\text{OC} <$  in the complex; the two electronic systems ( ${}^3\text{ROH}^*$  and  $\text{OC} <$ ) may be separated by a hydrogen bond between them. In contrast, for the excited singlet state a nonfluorescent CT state in the excited hydrogen-bonded pair is formed as reported by Mataga's group.<sup>32,33</sup> The difference in electronic structures between the excited singlet and triplet complexes may arise from the fact that in nature the electronic structure for the former state is ionic but the latter is not so ionic but radical-like. The triplet complex  ${}^3\text{ROH}^*\cdots\text{OC} <$  may dissociate into ROH and  $\text{OC} <$  when it decays to the ground state. Therefore, the  ${}^3\text{ROH}^*\cdots\text{OC} <$  complex can be called "a triplet exciplex".

At first, a transient kinetic treatment for the HT reaction has been made with a computer. The decay function  $F(t)$  of the transient absorbance at 430 nm for the triplet ROH species can be expressed as<sup>20,37</sup>

$$F(t) = c(e^{-\lambda_1 t} + Ae^{-\lambda_2 t}) \quad (6a)$$

where  $c$  denotes the constant and  $A = (X - \lambda_1)(\lambda_2 - X)^{-1}$ . The decay parameters  $\lambda_1$  and  $\lambda_2$  are

$$\lambda_{1,2} = \frac{1}{2}[X + Y \mp \{(Y - X)^2 + 4k_1k_2[>\text{CO}]\}^{1/2}] \quad (6b)$$

where  $X = \tau_0^{-1} + k_1[>\text{CO}]$  and  $Y = (\tau_0')^{-1} + k_{\text{HT}} + k_2$ . The formation of  ${}^3\text{ROH}^*$  is completed by  $t = 0.4 \mu\text{s}$  after laser pulsing. The observed decay function at 430 nm is, therefore, the same as that of eq 6a. The experimental value of  $\tau_0^{-1}$  ( $1.4 \times 10^5 \text{ s}^{-1}$ ) at 290 K was used. The values of  $k_1$ ,  $k_2$ , and  $(\tau_0')^{-1} [= (\tau_0')^{-1} + k_{\text{HT}}]$  were varied. With use of the values of  $\lambda_1$  and  $\lambda_2$  obtained

(36) Shizuka, H.; Fukushima, M., in preparation.

(37) Birks, J. B. "Photophysics of Aromatic Molecules"; John Wiley & Sons: London, 1970.

(32) Ikeda, N.; Okada, T.; Mataga, N. *Chem. Phys. Lett.* **1980**, *69*, 251. Ikeda, N.; Okada, T.; Mataga, N. *Bull. Chem. Soc. Jpn.* **1981**, *54*, 1025.

(33) Ikeda, N.; Miyasaka, H.; Okada, T.; Mataga, N. *J. Am. Chem. Soc.* **1983**, *105*, 5206 and references therein.

(34) Rehm, D.; Weller, A. *Isr. J. Chem.* **1970**, *8*, 259.

(35) Yamamoto, S.; Kikuchi, K.; Kokubun, H. *Bull. Chem. Soc. Jpn.* **1976**, *49*, 2950.

**Table III.** Kinetic Parameters for the Hydrogen Atom Transfer Reaction: Equilibrium Constants ( $K^*$ ) and Decay Rate Constants of Free  $^3\text{ROH}^*$  ( $\tau_0^{-1}$ ) and  $^3\text{ROH}^*\cdots\text{OC}<$  ( $(\tau')^{-1}$ )<sup>a,b</sup>

$T$ , K	$K^*$ , $\text{M}^{-1}$	$\tau_0^{-1}$ , $10^5 \text{ s}^{-1}$	$(\tau')^{-1}$ , <sup>c</sup> $10^6 \text{ s}^{-1}$	$k_{\text{HT}}$ , <sup>d</sup> $10^6 \text{ s}^{-1}$	$(\tau_0')^{-1}$ , $10^5 \text{ s}^{-1}$	$\phi_{\text{HT}}$ ' <sup>e</sup>
274	20.5 (20.5)	1.25	0.98 (0.98)	0.82 (0.82)	1.6 (1.6)	0.84 (0.84)
280	18.8 (18.8)	1.33	1.25 (1.26)	1.09 (1.09)	1.63 (1.67)	0.87 (0.87)
290	16.7 (16.6)	1.4	1.53 (1.52)	1.30 (1.29)	2.3 (2.3)	0.84 (0.85)
300	14.1 (14.7)	1.48	1.93 (1.87)	1.64 (1.57)	2.95 (3.01)	0.85 (0.84)
310	12.6 (12.8)	1.55	2.6 (2.6)	2.15 (2.15)	5.02 (5.0)	0.83 (0.83)
320	10.9 (10.9)	1.68	3.49 (3.48)	2.97 (2.97)	5.2 (5.12)	0.85 (0.85)

<sup>a</sup> Experimental errors within 5%. <sup>b</sup> Parentheses denote the values obtained from the Rayner–Wyatt plots. <sup>c</sup>  $(\tau')^{-1} = k_{\text{HT}} + (\tau_0')^{-1}$ . <sup>d</sup>  $k_{\text{HT}}$  denotes the rate constant for the hydrogen atom transfer reaction. <sup>e</sup>  $\phi_{\text{HT}}$ ' represents the hydrogen atom transfer efficiency for the formation of  $\text{RO}\cdot$  and  $>\text{COH}$  from the triplet complex:  $\phi_{\text{HT}}$ ' =  $k_{\text{HT}}x\tau'$ .

from eq 6b, fitting of the decay function  $F(t)$  was carried out. Figure 6a shows the typical observed and calculated results of the function  $F(t)$  at 290 K at the concentrations of  $>\text{CO}$ : (1)  $0.27 \times 10^{-2}$ , (2)  $0.667 \times 10^{-2}$ , and (3)  $1.0 \times 10^{-2}$  M. The best fitted values of  $\lambda_1$  and  $\lambda_2$  as a function of  $[>\text{CO}]$  are shown in Figure 6b. The values of  $k_1$ ,  $k_2$ , and  $(\tau')^{-1}$  were determined to be  $4.6 (\pm 0.4) \times 10^9 \text{ M}^{-1} \text{ s}^{-1}$ ,  $2.3 (\pm 0.3) \times 10^8 \text{ s}^{-1}$ , and  $1.7 (\pm 0.2) \times 10^6 \text{ s}^{-1}$ , respectively. The values of  $k_1$  and  $k_2$  are very much greater than those of the competitive processes [ $k_1 \gg \tau_0^{-1}$ ;  $k_2 \gg k_{\text{HT}} + (\tau_0')^{-1}$ ]. The value of  $K^*$  ( $=k_1/k_2$ ) is estimated to be about 20  $\text{M}^{-1}$ . That is, an equilibrium for the complex formation in Scheme II may be established. The existence of an isosbestic point at 500 nm in Figure 1b strongly supports Scheme II. The following equations proposed by Ware<sup>38</sup> and Rayner–Wyatt<sup>39</sup> can be applied to the present system, where the equilibrium is established during the lifetime in the excited state. The Ware equation reads

$$\{\tau_{\text{obsd}}^{-1} - \tau_0^{-1}\}^{-1} = \{(\tau')^{-1} - \tau_0^{-1}\}^{-1} \left\{ 1 + \frac{1}{K^*[\text{>CO}]} \right\} \quad (7)$$

The Rayner–Wyatt equation reads

$$\frac{1}{[\text{>CO}]} \{\tau_{\text{obsd}}^{-1} - \tau_0^{-1}\} = K^*(\tau')^{-1} - K^*\tau_{\text{obsd}}^{-1} \quad (8)$$

where  $\tau_{\text{obsd}}^{-1}$  denotes the observed decay rate of  $^3\text{ROH}^*$  monitored at 430 nm and  $(\tau')^{-1} = (\tau_0')^{-1} + k_{\text{HT}}$ . Both equations are essentially the same; in fact, if eq 9<sup>36</sup> is substituted into eq 8 one can derive the Ware equation (eq 7). The Rayner–Wyatt equation is very sensitive to the  $\tau_{\text{obsd}}$  value which appears on both sides in

$$(\tau_{\text{obsd}})^{-1} = \frac{\tau_0^{-1}}{1 + K^*[\text{>CO}]} + \frac{K^*[\text{>CO}](\tau')^{-1}}{1 + K^*[\text{>CO}]} \quad (9)$$

eq 8. The Ware equation is sensitive to  $[>\text{CO}]$ , since the difference between  $\tau_{\text{obsd}}^{-1}$  and  $\tau_0^{-1}$  becomes small at lower concentrations of  $[>\text{CO}]$ . The value of  $\tau_0^{-1}$  of the decay rate of  $^3\text{ROH}^*$  in the absence of  $>\text{CO}$  can be easily obtained from the intercept in Figure 5, since  $\tau_{\text{obsd}}^{-1}$  becomes  $\tau_0^{-1}$  at  $[>\text{CO}] \rightarrow 0$  as can be seen in eq 9. The values of  $\tau_0^{-1}$  at various temperatures obtained are listed in Table III. The Ware plot of  $(\tau_{\text{obsd}}^{-1} - \tau_0^{-1})^{-1}$  as a function of  $[>\text{CO}]^{-1}$  is shown in Figure 7a, and a straight line is obtained, demonstrating that the experimental results agree with

(38) Ware, W. R.; Watt, D.; Holmes, J. D. *J. Am. Chem. Soc.* **1974**, *96*, 7853.

(39) Rayner, D. M.; Wyatt, P. A. H. *J. Chem. Soc., Faraday Trans. 2* **1974**, *70*, 945.

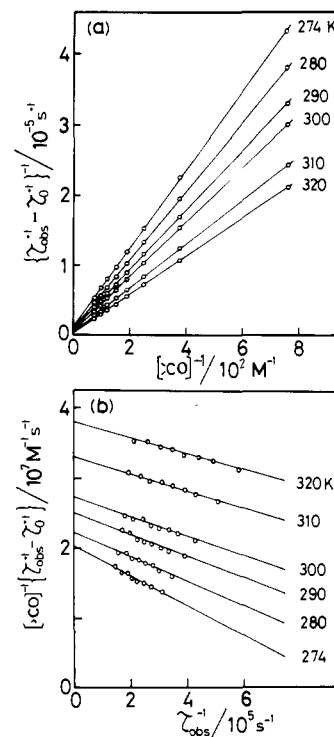


Figure 7. (a) The Ware plots of  $(\tau_{\text{obsd}}^{-1} - \tau_0^{-1})^{-1}$  vs.  $[>\text{CO}]^{-1}$  and (b) the Rayner–Wyatt plots  $[>\text{CO}]^{-1} (\tau_{\text{obsd}}^{-1} - \tau_0^{-1})$  vs.  $\tau_{\text{obsd}}^{-1}$  at various temperatures.

eq 7. The values of  $K^*$  and  $(\tau')^{-1}$  at 290 K obtained by the Ware plot are  $16.7 \text{ M}^{-1}$  and  $1.53 \times 10^6 \text{ s}^{-1}$ , respectively. The  $K^*$  value is almost the same as that (ca. 20  $\text{M}^{-1}$ ) obtained from  $k_1/k_2$  within 20% error.

Similarly, the values of  $K^*$  and  $(\tau')^{-1}$  at various temperatures obtained from the Ware plots are summarized in Table III. The Rayner–Wyatt plot of  $(\tau_{\text{obsd}}^{-1} - \tau_0^{-1}) [ >\text{CO}]^{-1}$  vs.  $\tau_{\text{obsd}}^{-1}$  is shown in Figure 7b, and a straight line is obtained. The values of  $K^*$  and  $(\tau')^{-1}$  obtained by the Rayner–Wyatt plots at various temperatures are also listed in Table III, which are about the same as those obtained by the Ware plots. The plots of  $\tau_{\text{obsd}}^{-1}$  [calculated from eq 9] vs.  $[\text{BP}]$  are shown by solid lines in Figure 5, which fit entirely the experimental results.

The  $k_{\text{HT}}$  value, which corresponds to the rate constant for the HT reaction from  $^3\text{ROH}^*\cdots\text{OC}<$  to  $\text{RO}\cdot$  plus  $>\text{COH}$ , can be estimated from the following equation:

$$k_{\text{HT}} = \frac{\Delta[>\text{COH}]}{\Delta[{}^3\text{ROH}^*\cdots\text{OC}<]} \tau_{\text{obsd}}^{-1} \quad (10)$$

where  $\Delta[>\text{COH}]$  denotes the change in the  $>\text{COH}$  concentrations between the delay times  $t_2$  and  $t_1$  and  $\Delta[{}^3\text{ROH}^*\cdots\text{OC}<]$  that in the concentrations of the triplet complex between  $t_1$  and  $t_2$ . The values of  $\Delta[>\text{COH}]$  and  $\Delta[{}^3\text{ROH}^*\cdots\text{OC}<]$  can be obtained from eq 11 and 12, respectively, where  $\Delta A_{545}$  represents the absorbance

$$\Delta[>\text{COH}] = \frac{\Delta A_{545}}{(\epsilon_{>\text{COH}})_{545} + (\epsilon_{\text{RO}\cdot})_{545}} \quad (11)$$

change at 545 nm between  $t_2$  and  $t_1$  and  $(\epsilon_{>\text{COH}})_{545}$  and  $(\epsilon_{\text{RO}\cdot})_{545}$  the molar extinction coefficients  $\epsilon$  of  $>\text{COH}$  and  $\text{RO}\cdot$  at 545 nm, whose values are 3220 and 830  $\text{M}^{-1} \text{ cm}^{-1}$ , respectively, as listed in Table I, where  $\Delta[{}^3\text{ROH}^*]$  and  $\Delta A_{430}$  denote respectively the

$$\Delta[{}^3\text{ROH}^*\cdots\text{OC}<] = \frac{K^*[\text{>CO}]}{1 + K^*[\text{>CO}]} \Delta[{}^3\text{ROH}^*] = \frac{K^*[\text{>CO}]}{1 + K^*[\text{>CO}]} \frac{\Delta A_{430}}{[(\epsilon_{\text{ROH}^*})_{430} - \{(\epsilon_{>\text{COH}})_{430} + (\epsilon_{\text{RO}\cdot})_{430}\}]} \quad (12)$$

change in the  $^3\text{ROH}^*$  concentrations and the absorbance change at 430 nm between  $t_1$  and  $t_2$ ,  $(\epsilon_{\text{ROH}^*})_{430}$ ,  $(\epsilon_{>\text{COH}})_{430}$ , and  $(\epsilon_{\text{RO}\cdot})_{430}$

the values of  ${}^3\text{ROH}^*$ ,  $>\dot{\text{C}}\text{OH}$ , and  $\text{RO}\cdot$  at 430 nm, respectively, which are listed in Table I. For instance,  $\Delta A_{545}$  and  $\Delta A_{430}$  were obtained to be  $7.5 \times 10^{-3}$  and  $3.3 \times 10^{-2}$ , respectively, at  $[>\text{CO}] = 6.67 \times 10^{-3}$  M at 290 K ( $K^* = 16.7 \text{ M}^{-1}$ ) by measurements of the corresponding absorbances at the delay times  $t_1 = 1 \mu\text{s}$  and  $t_2 = 2 \mu\text{s}$ . The values of  $\Delta[>\dot{\text{C}}\text{OH}]$ ,  $\Delta[{}^3\text{ROH}^*]$  and  $\Delta[{}^3\text{ROH}^*\cdots\text{OC}]$  are, therefore, evaluated to be  $1.86 \times 10^{-6}$ ,  $4.0 \times 10^{-6}$ , and  $4.01 \times 10^{-7}$  M, respectively. With use of these values, the  $k_{\text{HT}}$  value can be estimated to be  $1.3 \times 10^6 \text{ s}^{-1}$  at 290 K for the BP ( $6.67 \times 10^{-3}$  M) and ROH ( $3.0 \times 10^{-3}$  M) system from eq 10. The  $k_{\text{HT}}$  values obtained at various temperatures are summarized in Table III. The value of  $k_{\text{HT}}$  increases with increasing temperatures. The hydrogen atom transfer efficiency  $\phi_{\text{HT}}'$  for the formation  $>\dot{\text{C}}\text{OH}$  and  $\text{RO}\cdot$  from  ${}^3\text{ROH}^*\cdots\text{OC}$  is given by

$$\phi_{\text{HT}}' = k_{\text{HT}}\tau' \quad (13)$$

For example, the  $\phi_{\text{HT}}'$  value is determined to be 0.84 at 290 K, whose values obtained at various temperatures are summarized in Table III, and they are about 0.85 regardless of temperatures.

The values of  $(\tau_0')^{-1}$  can be determined from the equation  $(\tau_0')^{-1} = (\tau')^{-1} - k_{\text{HT}}$ , which are summarized in Table III. The  $(\tau_0')^{-1}$  values of the triplet complex is greater than that of  $\tau_0^{-1}$  of free  ${}^3\text{ROH}^*$ , suggesting that the nonradiative internal quenching may exist in the triplet complex as well as that in the excited singlet state of the hydrogen-bonded pair.<sup>32-35</sup>

The reaction quantum yield  $\Phi_{\text{HT}}$  for the HT reaction can be simply expressed as

$$\Phi_{\text{HT}} = \phi_{\text{ET}}\phi_{\text{HT}} \quad (14)$$

where  $\phi_{\text{ET}}$  denotes the T-T energy transfer efficiency from  ${}^3\text{BP}^*$  to ROH and  $\phi_{\text{HT}}$  the HT reaction efficiency for the formation of  $>\dot{\text{C}}\text{OH}$  and  $\text{RO}\cdot$  from  ${}^3\text{ROH}^*$  which can be represented as  $\phi_{\text{HT}} = K^*[>\text{CO}]\{1 + K^*[>\text{CO}]\}^{-1}k_{\text{HT}}\tau_{\text{obsd}}$ . The values of  $\phi_{\text{ET}}$ ,  $K^*$ ,  $k_{\text{HT}}$ , and  $\tau_{\text{obsd}}$  are 0.58,  $16.7 \text{ M}^{-1}$ ,  $1.3 \times 10^6 \text{ s}^{-1}$ , and  $3.6 \times 10^{-6}$  s, respectively, for the BP ( $6.67 \times 10^{-3}$  M) and ROH ( $3.0 \times 10^{-3}$  M) system at 290 K as described above. The value of  $\phi_{\text{HT}}$  can be obtained to be 0.47, which agrees well with that (0.48) obtained by the spectral change in Figure 1b within the experimental error. On the basis of kinetics the  $\Phi_{\text{HT}}$  value can be determined to be 0.27, which is in accordance with that (0.28) obtained by the spectral change in Figure 1 as stated above.

Thus, it can be said that the hydrogen atom transfer from  ${}^3\text{ROH}^*$  (sensitized by  ${}^3\text{BP}^*$ ) to the ground BP occurs effectively on the basis of the kinetic treatments. The HT reaction is completed in  $\sim 7 \mu\text{s}$  at 290 K. It should be noted that no excited-state proton transfer of ROH<sup>40</sup> takes place for the present system. The fate of the radicals  $\text{RO}\cdot$  and  $>\dot{\text{C}}\text{OH}$  is the decay mainly via the radical reaction between them, as described above. The rate constant  $k_{\text{r}}$  in Scheme II can be obtained to be  $1.7 \times 10^9 \text{ M}^{-1} \text{ s}^{-1}$  at 290 K from the second-order kinetics in Figure 4b by using the  $\epsilon$  values of  $\text{RO}\cdot$  ( $830 \text{ M}^{-1} \text{ cm}^{-1}$ ) and  $>\dot{\text{C}}\text{OH}$  ( $3220 \text{ M}^{-1} \text{ cm}^{-1}$ )<sup>23</sup> and the maximum concentrations of  $>\dot{\text{C}}\text{OH}$  and  $\text{RO}\cdot$  ( $8.6 \times 10^{-6}$  M and  $6.1 \times 10^{-6}$  M at the delay time =  $7 \mu\text{s}$  at 290 K, respectively). The radical combination rate between  $\text{RO}\cdot$  and  $>\dot{\text{C}}\text{OH}$  is very much faster than that between the ketyl radicals.

**Temperature Effects on the Kinetic Parameters  $K^*$ ,  $k_{\text{HT}}$ ,  $\tau_0^{-1}$ , and  $(\tau_0')^{-1}$ .** The plot of  $K^*$  vs.  $T^{-1}$  is shown in Figure 8a, and from the van't Hoff equation the enthalpy change  $\Delta H^*$  and the entropy change  $\Delta S^*$  for formation of the triplet complex in Scheme II are obtained to be  $-2.4 \text{ kcal mol}^{-1}$  and  $-2.7 \text{ eu}$ , respectively. The complex formation is an exothermic reaction (e.g., the free energy change  $\Delta G^*$  is  $-1.6 \text{ kcal mol}^{-1}$  at 290 K).

The plots of  $k_{\text{HT}}$ ,  $\tau_0^{-1}$ , and  $(\tau_0')^{-1}$  as a function of  $T^{-1}$  are depicted in Figure 8b. On the assumptions that these processes follow the Arrhenius relation, both frequency factors ( $A_{\text{HT}}$ ,  $A_0$ , and  $A_0'$ , respectively) and activation energies ( $\Delta E_{\text{HT}}$ ,  $\Delta E_0$ , and  $\Delta E_0'$ , respectively) are determined from Figure 8b, whose values are listed in Table IV. For the HT reaction with both the

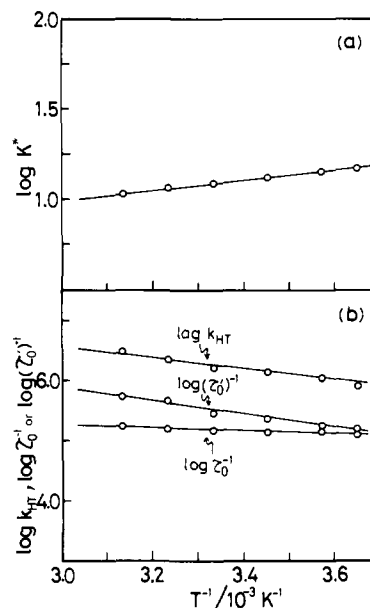


**Figure 8.** (a) The van't Hoff plot of  $\log K^*$  vs.  $T^{-1}$  and (b) the Arrhenius plots of  $\log k_{\text{HT}}$ ,  $\log \tau_0^{-1}$ , and  $\log (\tau_0')^{-1}$  vs.  $T^{-1}$ .

**Table IV.** Thermodynamic and Activation Parameters for the Hydrogen Atom Transfer Reaction<sup>a</sup>

$K^*$		$k_{\text{HT}}$		$\tau_0^{-1}$		$(\tau_0')^{-1}$	
$\Delta H^*$ , <sup>b</sup>	$\Delta S^*$ , <sup>b</sup>	$A_{\text{HT}}$ , <sup>b</sup>	$\Delta E_{\text{HT}}$ , <sup>c</sup>	$A_0$ , <sup>c</sup>	$\Delta E_0$ , <sup>d</sup>	$A_0'$ , <sup>b</sup>	$\Delta E_0'$ , <sup>d</sup>
kcal	eu	$10^9 \text{ s}^{-1}$	kcal	$10^9 \text{ s}^{-1}$	kcal	$10^9 \text{ s}^{-1}$	kcal
mol <sup>-1</sup>			mol <sup>-1</sup>		mol <sup>-1</sup>		mol <sup>-1</sup>
-2.4	-2.7	3.7	4.6	8.47	1.04	1.57	5.06

<sup>a</sup>Data taken from the Ware plots. <sup>b</sup> $\Delta H^*$  and  $\Delta S^*$  denote the enthalpy change and entropy change, respectively, for the equilibrium constant  $K^*$ . <sup>c</sup> $A_{\text{HT}}$ ,  $A_0$ , and  $A_0'$  represent frequency factors for the  $k_{\text{HT}}$ ,  $\tau_0^{-1}$ , and  $(\tau_0')^{-1}$  processes, respectively. <sup>d</sup> $\Delta E_{\text{HT}}$ ,  $\Delta E_0$ , and  $\Delta E_0'$  are activation energies for the  $k_{\text{HT}}$ ,  $\tau_0^{-1}$ , and  $(\tau_0')^{-1}$  processes, respectively.

apparent frequency  $A_{\text{HT}}$  ( $3.7 \times 10^9 \text{ s}^{-1}$ ) and activation energy  $\Delta E_{\text{HT}}$  ( $4.6 \text{ kcal mol}^{-1}$ ), a theoretical analysis according to the golden rule treatment<sup>41,42</sup> or the treatment of radiationless transition<sup>10,11</sup> will be needed in the future. Probably, the HT reaction may proceed via a tunneling process. It is shown that the present HT reaction from  ${}^3\text{ROH}^*$  to BP does not occur directly but proceeds through the triplet complex  ${}^3\text{ROH}^*\cdots\text{OC}$ . This system may be convenient to estimate a molecular conformation of the complex for the theoretical analysis.

## Conclusion

It is found that the hydrogen atom transfer reaction from 1-naphthol triplet (produced by triplet sensitization of benzophenone) to ground benzophenone occurs effectively via the triplet complex  ${}^3\text{ROH}^*\cdots\text{OC}$  to give the naphthoxy radical  $\text{RO}\cdot$  and the ketyl radical  $>\dot{\text{C}}\text{OH}$ . The triplet-triplet energy transfer  $k_{\text{ET}}$  ( $4.1 \times 10^9 \text{ M}^{-1} \text{ s}^{-1}$ ) from  ${}^3\text{BP}^*$  to ROH is competitive with both the usual hydrogen atom abstraction  $k_{\text{HA}}$  ( $7.4 \times 10^8 \text{ M}^{-1} \text{ s}^{-1}$ ) of  ${}^3\text{BP}^*$  from ROH and the quenching  $k_q'$  ( $2.2 \times 10^9 \text{ M}^{-1} \text{ s}^{-1}$ ) of  ${}^3\text{BP}^*$  induced by ROH in methanol at 290 K, whose efficiencies are 0.58, 0.11, and 0.31, respectively. These primary processes of  ${}^3\text{BP}^*$  are completed in 300 ns, and subsequently the equilibrium  ${}^3\text{ROH}^* + >\text{CO} \rightleftharpoons {}^3\text{ROH}^*\cdots\text{OC}$  is established very quickly. The equilibrium constant  $K^*$  for the triplet complex formation is obtained to be  $16.7 \text{ M}^{-1}$  at 290 K ( $\Delta H^* = -2.4 \text{ kcal mol}^{-1}$  and  $\Delta S^* = -2.7 \text{ eu}$ ). The hydrogen atom transfer reaction  $k_{\text{HT}}$  takes place via  ${}^3\text{ROH}^*\cdots\text{OC}$  with the rate constant ( $1.3 \times 10^6 \text{ s}^{-1}$  at 290 K,  $A_{\text{HT}} = 3.7 \times 10^9 \text{ s}^{-1}$ ;  $\Delta E_{\text{HT}} = 4.6 \text{ kcal mol}^{-1}$ ), which is

(41) Siebrand, W.; Wildman, T. A.; Zgierski, M. Z. *J. Am. Chem. Soc.* **1984**, *106*, 4083.

(42) Siebrand, W.; Wildman, T. A.; Zgierski, M. Z. *J. Am. Chem. Soc.* **1984**, *106*, 4089.

(40) E.g.: Tsutsumi, K.; Shizuka, H. *Z. Phys. Chem. (Wiesbaden)* **1980**, *122*, 129.

completed in  $\sim 7 \mu\text{s}$ . The efficiency  $\phi_{\text{HT}}$  from the triplet complex to yield  $\text{RO}\cdot$  and  $>\dot{\text{C}}\text{OH}$  is large ( $\sim 0.85$ ) regardless of temperatures. Both  $\text{RO}\cdot$  and  $>\dot{\text{C}}\text{OH}$  produced by laser flash photolysis decay mainly via the radical recombination  $k_{\text{R}}$  between them with the rate constant  $1.7 \times 10^9 \text{ M}^{-1} \text{ s}^{-1}$ . The reaction mechanism for the hydrogen atom transfer reaction of  ${}^3\text{ROH}^*$

(produced by the triplet sensitization of BP) is shown in Schemes I and II.

**Acknowledgment.** The authors are very grateful to Professor P. J. Wagner of Michigan State University for his helpful suggestions and stimulating discussion.

## Stereodynamics of a Series of Di-*tert*-butylphosphines [(*t*-C<sub>4</sub>H<sub>9</sub>)<sub>2</sub>PR; R = H, CH<sub>3</sub>, C<sub>2</sub>H<sub>5</sub>, CH<sub>2</sub>C<sub>6</sub>H<sub>5</sub>, *i*-C<sub>3</sub>H<sub>7</sub>, *t*-C<sub>4</sub>H<sub>9</sub>, and C<sub>6</sub>H<sub>5</sub>]. Carbon-13, Proton, and Phosphorus-31 NMR Studies. Molecular Mechanics Calculations

Christopher D. Rithner\* and C. Hackett Bushweller\*

Contribution from the Department of Chemistry, University of Vermont, Burlington, Vermont 05405. Received April 18, 1985

**Abstract:** A series of di-*tert*-butylphosphines [(*t*-C<sub>4</sub>H<sub>9</sub>)<sub>2</sub>PR; R = H, CH<sub>3</sub>, C<sub>2</sub>H<sub>5</sub>, CH<sub>2</sub>C<sub>6</sub>H<sub>5</sub>, *i*-C<sub>3</sub>H<sub>7</sub>, *t*-C<sub>4</sub>H<sub>9</sub>, and C<sub>6</sub>H<sub>5</sub>] has been studied by variable-temperature <sup>1</sup>H, <sup>13</sup>C{<sup>1</sup>H}, and <sup>31</sup>P{<sup>1</sup>H} NMR spectroscopy. In all cases, the <sup>31</sup>P{<sup>1</sup>H} spectrum remains a singlet down to 110 K. With the exception of (*t*-C<sub>4</sub>H<sub>9</sub>)<sub>2</sub>PH, <sup>1</sup>H and <sup>13</sup>C{<sup>1</sup>H} spectra show a decoalescence due to slowing *tert*-butyl rotation. For (*t*-C<sub>4</sub>H<sub>9</sub>)<sub>3</sub>P, <sup>13</sup>C{<sup>1</sup>H} spectra display two separate decoalescence phenomena over different temperature ranges. These are attributed to *tert*-butyl rotation ( $\Delta G^\ddagger = 8.9 \text{ kcal/mol}$ ) and to libration of twisted *tert*-butyl groups ( $\Delta G^\ddagger = 5.9 \text{ kcal/mol}$ ), which effects racemization of C<sub>3</sub>-symmetric equilibrium enantiomers. The <sup>13</sup>C{<sup>1</sup>H} spectrum of (*t*-C<sub>4</sub>H<sub>9</sub>)<sub>2</sub>P(*i*-C<sub>3</sub>H<sub>7</sub>) at 110 K reveals a strong preference for that conformation having one isopropyl methyl group oriented anti and the other gauche to the phosphorus lone pair, as well as a *tert*-butyl rotation barrier ( $\Delta G^\ddagger = 6.7 \text{ kcal/mol}$ ) which is higher than the isopropyl rotation barrier ( $\Delta G^\ddagger = 4.8 \text{ kcal/mol}$ ). Both <sup>1</sup>H and <sup>13</sup>C{<sup>1</sup>H} spectra of (*t*-C<sub>4</sub>H<sub>9</sub>)<sub>2</sub>PC<sub>6</sub>H<sub>5</sub> suggest an equilibrium conformation in which the phenyl plane bisects the CPC bond angle associated with the two *tert*-butyl groups, and the spectra also reveal a relatively high barrier to 2-fold phenyl rotation ( $\Delta G^\ddagger = 10.5 \text{ kcal/mol}$ ) as compared to *tert*-butyl rotation ( $\Delta G^\ddagger = 6.3 \text{ kcal/mol}$ ). For all seven phosphines, molecular mechanics calculations predict equilibrium conformations with twisted *tert*-butyl groups. For those phosphines in which R  $\neq$  H, the molecular mechanics calculations also predict a twist about the P-R bond. The *tert*-butyl and P-R twisting result presumably from optimization of repulsions between proximate groups which are bonded to the ends of C-P-C linkages. For R = C<sub>2</sub>H<sub>5</sub> and CH<sub>2</sub>C<sub>6</sub>H<sub>5</sub>, the molecular mechanics calculations predict a strong preference of the C<sub>2</sub>H<sub>5</sub> methyl and CH<sub>2</sub>C<sub>6</sub>H<sub>5</sub> phenyl groups for positions gauche and not anti to the lone pair. For all these phosphines, molecular mechanics predicts *tert*-butyl rotation barriers which are higher than libration (twisting) barriers. For R = CH<sub>3</sub>, C<sub>2</sub>H<sub>5</sub>, CH<sub>2</sub>C<sub>6</sub>H<sub>5</sub>, *i*-C<sub>3</sub>H<sub>7</sub>, and C<sub>6</sub>H<sub>5</sub>, the NMR spectrum recorded at the lowest temperature which allowed a meaningful spectrum (ca. 110 K) is consistent with *slow tert*-butyl rotation and *rapid* libration on the NMR time scale which agrees with molecular mechanics predictions of libration barriers too low to be NMR-accessible. For (*t*-C<sub>4</sub>H<sub>9</sub>)<sub>3</sub>P, molecular mechanics predicts C<sub>3</sub>-symmetric equilibrium enantiomers with both *tert*-butyl and libration barriers high enough to be NMR-accessible. <sup>13</sup>C{<sup>1</sup>H} spectra show two decoalescence phenomena attributed to both processes.

Amines and phosphines constitute two important classes of chemical compounds which possess a tricoordinate, pyramidal central atom. In attempting to elucidate the stereodynamics of secondary or tertiary amines and phosphines, one must remain cognizant of pyramidal inversion at the tricoordinate center, isolated rotation about the bonds to nitrogen or phosphorus, and twisting about the bonds to the central atom in response to steric crowding.

In amines, the inversion barrier and pyramidality at nitrogen vary over a wide range and can be a function of N-substituent  $\pi$ -bonding, N-substituent electronegativity, steric crowding, and ring strain.<sup>1</sup> Nitrogen inversion barriers and isolated rotation barriers about carbon-nitrogen bonds can be comparable, and care must be taken in interpreting dynamic NMR (DNMR) spectra.<sup>2,3</sup>

In contrast, inversion barriers in phosphines are high ( $>25 \text{ kcal/mol}$ ),<sup>1,4</sup> while isolated rotation barriers about carbon-phosphorus bonds are generally substantially lower. The rotation/inversion dichotomy in phosphines is clear-cut.<sup>5-14</sup>

(1) (a) Rauk, A.; Allen, L. C.; Mislow, K. *Angew. Chem., Int. Ed. Engl.* **1970**, *9*, 400. (b) Lambert, J. B. *Top. Stereochem.* **1971**, *6*, 19. (c) Raban, M.; Greenblatt, J. "The Chemistry of Amino, Nitroso, and Nitrocompounds and Their Derivatives"; Patai, S., Ed.; Wiley: New York, 1982; Part 1, pp 53-83.

(2) (a) Bushweller, C. H.; Fleischman, S. H.; Grady, G. L.; McGoff, P.; Rithner, C. D.; Whalon, M. R.; Brennan, J. G.; Marcantonio, R. P.; Domingue, R. P. *J. Am. Chem. Soc.* **1982**, *104*, 6224. (b) Fleischman, S. H.; Whalon, M. R.; Rithner, C. D.; Grady, G. L.; Bushweller, C. H. *Tetrahedron Lett.* **1982**, *23*, 4233.

(3) Bushweller, C. H.; Anderson, W. G.; Stevenson, P. E.; Burkey, D. L.; O'Neil, J. W. *J. Am. Chem. Soc.* **1974**, *96*, 3892.

(4) (a) Mislow, K. *Trans. N.Y. Acad. Sci.* **1973**, *35*, 227. (b) Baechler, R. D.; Mislow, K. *J. Am. Chem. Soc.* **1970**, *92*, 3090.

(5) (a) Kojima, T.; Breig, E. L.; Lin, C. C. *J. Chem. Phys.* **1961**, *35*, 2139. (b) Nelson, R. *Ibid.* **1963**, *39*, 2382. (c) Lide, D. R.; Cox, A. W., Jr. *Ibid.* **1976**, *64*, 1930.

(6) (a) Bartell, L. S. *J. Chem. Phys.* **1960**, *32*, 832. (b) Bartell, L. S.; Brockway, L. O. *Ibid.* **1960**, *32*, 512.

(7) (a) Durig, J. R.; Cox, A. W., Jr. *J. Chem. Phys.* **1975**, *63*, 2303. (b) Durig, J. R.; Cox, A. W., Jr. *Ibid.* **1976**, *80*, 2493. (c) Durig, J. R.; Cox, A. W., Jr. *J. Mol. Struct.* **1977**, *38*, 77.

(8) (a) Bushweller, C. H.; Brunelle, J. A. *J. Am. Chem. Soc.* **1973**, *95*, 5949. (b) Robert, J. B.; Roberts, J. D. *Ibid.* **1972**, *94*, 4902.

(9) (a) Bushweller, C. H.; Brunelle, J. A. *Tetrahedron Lett.* **1974**, *11*, 893. (b) Schmidbaur, H.; Blaschke, G.; Kohler, F. H. *Z. Naturforsch., B* **1977**, *32b*, 757. (c) Bushweller, C. H.; Lourandos, M. *Z. Inorg. Chem.* **1974**, *13*, 2514.

(10) Wroczynski, R. J.; Mislow, K. *J. Am. Chem. Soc.* **1979**, *101*, 3980.

(11) Bushweller, C. H.; Anderson, W. G.; Stevenson, P. E.; O'Neil, J. W. *J. Am. Chem. Soc.* **1975**, *97*, 4338.

(12) (a) Seymour, S. J.; Jonas, T. *J. Magn. Reson.* **1972**, *8*, 376. (b) Seymour, S. J.; Jonas, J. *J. Chem. Phys.* **1971**, *54*, 487.